AIAA JOURNAL
Vol. 38, No. 8, August 2000

Modeling the Response from a Cascade to an Upstream Acoustic Disturbance

Gerald C. Paynter* and Larry T. Clark†
The Boeing Company, Seattle, Washington 98124
and
Gary L. Cole‡
NASA John H. Glenn Research Center at Lewis Field, Cleveland, Ohio 44135

Time-accurate Euler simulations for the flow through a two-dimensional cascade subjected to an upstream acoustic disturbance were used as the basis for a small-disturbance model to predict the reflected response upstream of the cascade. The small-disturbance model results in a linear system of algebraic equations for the properties of the reflected and transmitted disturbances. The model predicts the reflected and transmitted responses as a function of the cascade blade geometry, the disturbance amplitude, and the initial flow properties. A new characteristic outflow boundary condition based on the small-disturbance response model was formulated and demonstrated independently in two one-dimensional Euler codes. The new boundary condition was found to provide a significant improvement in accuracy for the reflection response of an acoustic disturbance from a compressor relative to existing outflow boundary-condition models.

Nomenclature

a	= local sonic velocity
C	= blade chord length
C_v	= specific heat at constant volume
e	= internal energy per unit mass
M, M_{x1}	= initial axial Mach number
p	= local static pressure, Pa or N/m^2
q, r, s,	= Riemann invariants
R	= response coefficient, β
S	= blade spacing
T	= static temperature
t	= time
u	= axial velocity
X	= axial coordinate direction, inches or 0.03882 m
Y	= coordinate in direction of blade motion, inches or 0.03882 m
Γ	= stagger angle
γ	= ratio of specific heats
Δt	= time step, $t^{n+1} - t^n$
Δx	= spatial step, $x_i - x_{i-1}$
ρ	= density
σ	= Courant number
$\bar{\sigma}$	= solidity, C/S

Subscripts

i	= spatial grid point at the outflow boundary
$i-1$	= spatial grid point one cell from the outflow boundary
t, x	= differentiation with respect to these variables
1, 2, 3, 4	= flow regions defined by Figs. 4 and 5

Superscripts

n	= current time step
$n+1$	= new time step

Received 13 November 1997; presented as Paper 98-0953 at the AIAA 36th Aerospace Sciences Meeting, Reno, NV, 12–15 January 1998; revision received 24 May 1999; accepted for publication 7 February 2000.

*Boeing Technical Fellow, MS 67-LF, P.O. Box 3707, Commercial Airplane Group. Associate Technical Fellow AIAA.
†Boeing Technical Fellow, MS 67-LF, P.O. Box 3707, Commercial Airplane Group.
‡Senior Research Engineer, MS 5-11, Research and Technology Directorate, 21000 Brookpark Road.

Introduction

SUPERSONIC aircraft encounter atmospheric disturbances while in flight. If the propulsion system uses a mixed compression inlet to decelerate and compress the captured airflow for the engine, these disturbances can cause the shock system to be expelled from the inlet. This event is known as an inlet unstart. An unstart results in a serious loss of propulsive efficiency and can cause an asymmetric loading of the wing that could require large control surface forces to maintain aircraft control.

An atmospheric disturbance encounter is thought to result in acoustic and convective disturbances to the inlet flow. Acoustic disturbances are pressure disturbances that propagate downstream through the inlet at the local velocity plus the local speed of sound. Convective disturbances are temperature and density changes without an associated pressure change, or velocity changes without an associated pressure change (a vorticity disturbance) that propagate downstream through the inlet at the local stream velocity. Both acoustic and convective disturbances eventually pass through the inlet and interact with the compressor.

Mixed compression supersonic inlets are designed to avoid inlet unstart due to atmospheric and engine-generated disturbances. The throat boundary-layer bleed system, throat slots, and flow bypass systems; the inlet control system; the design value of the throat Mach number; and the position of the normal shock relative to the inlet throat are all used to achieve a sufficient stability margin to prevent unstart. Inlet stability measures, however, increase the inlet performance penalty, weight, complexity, and cost.

Time-accurate Euler/Navier–Stokes (ENS) simulations of the inlet flow subjected to disturbances are now being used to support the design of mixed compression inlets.[1,2] One goal of this analysis is to support the design of an inlet with a desired stability margin (unstart tolerance) while minimizing the performance penalty. Time-accurate ENS simulations of inlet flows are used to explore parametric variations of design parameters that affect inlet stability. The accuracy and, therefore, the usefulness of the ENS simulations depend on the accuracy of the boundary conditions used in the simulation. At the compressor face, the flow is subsonic. When acoustic and convective disturbances interact with the first stage of the compressor, reflected and transmitted disturbances result from this interaction. The reflected disturbance propagates back toward the inlet throat and can cause the inlet to unstart. The transmitted disturbances travel downstream through the compressor blade passages, interact with the next compressor stage, and generate reflected and transmitted disturbances throughout the later stages of the compressor.

The speed and memory available with current computers are insufficient to support the ENS simulation of the inlet/engine combination (at least in the context of a design study). Thus, the effect of the engine on the inlet flow is simulated through the selection of a boundary condition (the compressor-face boundary condition) for unsteady time-accurate inlet flow analyses to investigate inlet stability issues. A number of compressor-face boundary-condition hypotheses have been put forward by various investigators.[3–7] A physical experiment[8,9] has been completed for evaluation of compressor-face boundary-condition hypotheses.

A time-accurate numerical study, performed with the NPARC[10] computer code, was recently reported[11] that investigated the interaction of acoustic and convective temperature disturbances with an unstalled cascade. The study provides details of the response of the flow as a function of the disturbance, the upstream flow properties, and the blade geometry. The purpose of the present paper is to provide a small-disturbance model for the flow through a two-dimensional cascade subjected to an upstream acoustic disturbance, that is based on the simulations of Ref. 11 and to put forward a new outflow boundary condition that utilizes the model. Model results are then compared with the Euler simulation results[11] and with experimental results.[8,9] The new boundary condition is then demonstrated independently in two one-dimensional Euler codes[12,13] and the predicted results compared with the results from a compressor experiment and with predicted results using existing boundary conditions. Finally, results from a one-dimensional Euler simulation of a supersonic mixed-compression inlet are presented as an example application, using new and existing boundary conditions. The dependence of inlet normal-shock response and unstart tolerance on the outflow boundary condition is demonstrated.

Flowfield Observations for an Acoustic Disturbance

For step acoustic disturbances, a parametric numerical study[11] was conducted to determine the amplitude of the reflected disturbance in the region upstream of the blade face as a function of the blade solidity, stagger angle, axial Mach number, blade loading, camber, and acoustic disturbance strength. For flat and unloaded blades, stagger angles of 20, 45, and 70 deg were considered at axial Mach numbers of 0.3 and 0.5. For blade solidities greater than one, the amplitude of the reflected disturbance was found to be independent of solidity. The initial acoustic disturbance was a step increase in static pressure.

The effects of stagger angle and upstream Mach number on the pressure increase of the reflected disturbance for an unloaded blade with a blade solidity of 1.0 are shown in Fig. 1. The initial upstream disturbance was a step change in pressure with $\delta p/p = 0.01$. The amplitude of the reflected disturbance was found to increase with increasing stagger angle and increasing upstream axial Mach number.

The effect of blade loading was investigated by assuming a typical initial angle of attack of the initial flow, relative to the blading, over the range of stagger angles noted earlier for axial Mach numbers of 0.3 and 0.5. Blade loading was found to have a weak effect on the strength of the reflected disturbance.

Euler analyses using the Ref. 11 analysis technique and assuming an unloaded blade (blade loading increased the computer time to achieve a steady-state solution prior to the introduction of a disturbance) were used to explore in greater detail the interaction of an acoustic disturbance with a cascade. This led to the following observations about the interaction. These observations are the basis for the small-disturbance response model proposed later.

1) The process for turning the flow to align it with the blade passage is dependent on whether the flow prior to the disturbance is subsonic or supersonic relative to the blade in a blade frame of reference. The subsonic process is illustrated in Fig. 2, and the supersonic process is illustrated in Fig. 3. The axial Mach number for the subsonic process of Fig. 2 was 0.28. The axial Mach number for the supersonic process of Fig. 3 was 2.05. The stream traces for the subsonic process show that the turning to align the flow with the blade passage starts with the reflected disturbance and is completed well into the blade passage. If the flow is supersonic (Fig. 3) all of the turning to align the flow with the blade passage occurs through the reflected disturbance upstream of the blade passage.

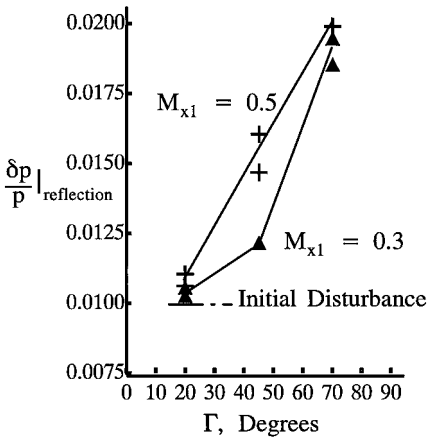

Fig. 1 Euler simulation results showing the effects of M_{x1} and Γ on the amplitude of the reflected disturbance.

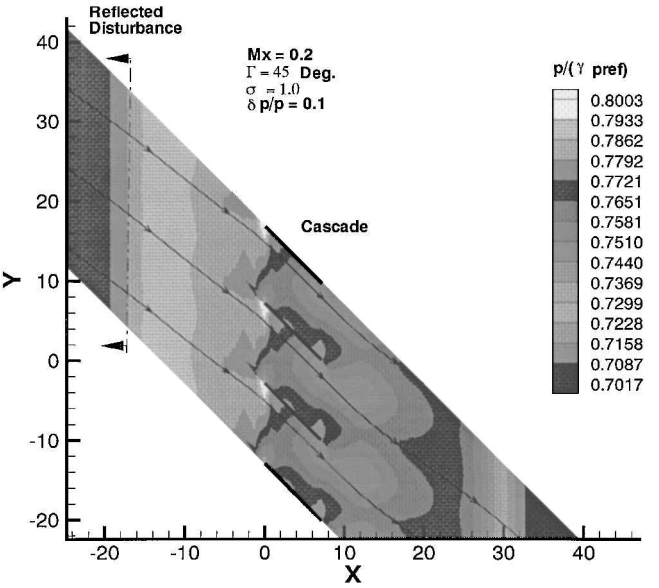

Fig. 2 Reflection of an acoustic disturbance with a subsonic blade passage Mach number.

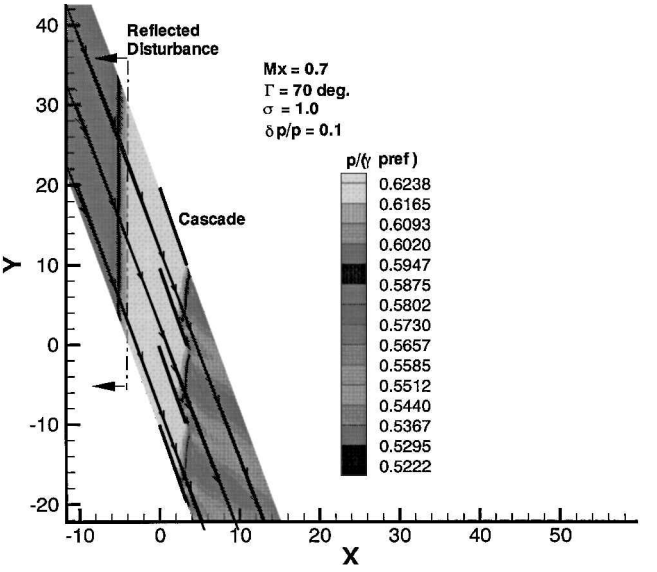

Fig. 3 Reflection of an acoustic disturbance with a supersonic blade passage Mach number.

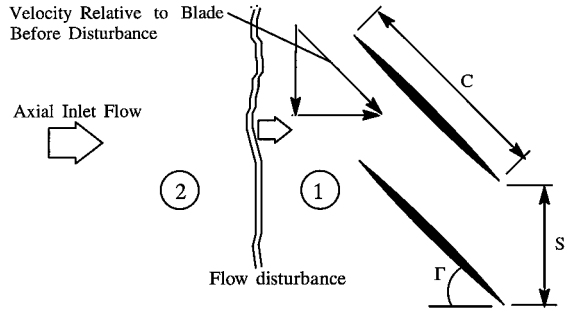

Fig. 4 Flow schematic prior to the disturbance: disturbance approaches the blade pair from the left.

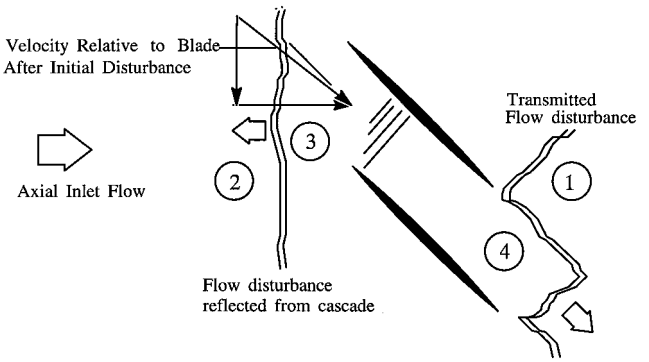

Fig. 5 Flow schematic after the disturbance interaction: reflected disturbance travels upstream to the left.

2) For both subsonic and supersonic Mach numbers, the initial acoustic disturbance results in two disturbances after the interaction with the cascade: a reflected, left-running acoustic disturbance that propagates upstream and a transmitted, right-running acoustic disturbance that propagates downstream.

3) For a subsonic initial Mach number, four distinct flow regions were identified from the Euler simulations. These are denoted by the circled numbers in Figs. 4 and 5. The flow properties in region 1 are those prior to any disturbance. The flow properties in region 2 are those just after the downstream propagating acoustic disturbance. The flow properties in region 3 are those between the cascade leading edge and the upstream propagating reflected disturbance. The flow properties in region 4 are those between the downstream face of the cascade and the transmitted disturbance.

4) For the right-running initial disturbance (Fig. 4) a step increase in pressure causes an increase in the axial velocity between regions 1 and 2. The tangential component of velocity is unchanged between regions 1 and 2. This means that the flow in region 2 is no longer aligned with the cascade. The changes in static flow properties between regions 1 and 2 are isentropic. The total pressure and temperature of regions 1 and 2 are, however, different because these regions are separated by a right-running acoustic wave.

5) The tangential component of velocity is, once again, unchanged (between regions 2 and 3). The reflected disturbance is a plane wave propagating upstream in the axial direction that changes only the axial component of velocity. The changes in static properties across the reflected wave are also isentropic.

6) The axial component of velocity is decreased between regions 2 and 3. This decrease in axial velocity partially aligns the flow with the blade passage.

7) Final alignment of the flow with the blade passage occurs in the blade passage between regions 3 and 4. The changes in static properties between regions 4 and 1 across the transmitted disturbance are also isentropic.

8) The flow in region 4 is aligned with the blade passage. Because the flow in region 1 into which the transmitted disturbance will propagate is also aligned, the transmitted disturbance must propagate along the blade passage. This induces changes in both the axial and tangential components of velocity to maintain the alignment of the flow with the blade passage.

Small Disturbance Model for the Acoustic Disturbance/Blade Interaction

If an analysis model of the reflection of an acoustic disturbance from a cascade is to be useful in an outflow boundary condition, it must satisfy two conditions. First, the model must predict the amplitude of the reflected disturbance accurately as a function of the upstream flow properties, the blade geometry, and the initial disturbance amplitude. Second, the model must be simple enough to be practical to implement in an outflow boundary condition.

Subsonic Mach Number

The flows in regions 3 and 4 can interact through the blade passage. The goal of the small-disturbance model is to relate the flow properties in regions 1–4 just after the interaction of the acoustic disturbance with the cascade as illustrated in Fig. 5. Following Shapiro,[14] it is assumed that the squares and products of perturbation terms are negligible in the equations used to relate the flow properties in regions 1–4.

In addition to the preceding flow observations, the following assumptions are made:

1) The flow properties prior to the disturbance (region 1) are known.

2) The cascade blade geometry is a flat plate of zero thickness and with a solidity greater than one.

3) The cascade is initially unloaded; the flow prior to the disturbance is aligned with the blade passage.

4)The disturbance is a step change in static pressure of known amplitude.

Shapiro[14] derives the following relationships for the motion of a wave of small amplitude following a small-perturbation analysis approach. For a right-running wave in a constant area flow with an initial velocity U in the direction of wave propagation,

$$\frac{\delta p}{p} = \gamma \frac{\delta U}{a} = \gamma M \frac{\delta U}{U} \tag{1}$$

where a is the local sonic velocity. For a left-running wave,

$$\frac{\delta p}{p} = -\gamma \frac{\delta U}{a} = -\gamma M \frac{\delta U}{U} \tag{2}$$

The small-disturbance model is developed by writing a system of flow equations relating the flow properties in regions 1–4 of Fig. 5. Using region 1 as a reference state and noting that the subscript denotes the properties in a given flow region, we have, in small-disturbance notation,

$$p_2 = p_1 + p_2', \qquad u_2 = u_1 + u_2'$$

Across the initial disturbance, from Eq. (1),

$$\frac{\delta p}{p_1} = \frac{p_2 - p_1}{p_1} = \frac{p_2'}{p_1}$$

Similarly,

$$\delta u / u_1 = u_2' / u_1$$

Using Eq. (1), we have

$$p_2' / p_1 = \gamma M_{x1} (u_2' / u_1) \tag{3}$$

Using Eq. (2) and following a similar development for the left-running reflected disturbance yields

$$p_3' / p_1 - p_2' / p_1 = -\gamma M_{x1} (u_3' / u_1) + \gamma M_{x1} (u_2' / u_1) \tag{4}$$

Substituting Eq. (3) into Eq. (4) and rearranging yields

$$p_3' / p_1 + \gamma M_{x1} (u_3' / u_1) = 2 (p_2' / p_1) \tag{5}$$

Writing a continuity equation for a control volume about the cascade blade passage (neglecting the storage effect of the blade passage volume) yields

$$\rho_3 u_3 = \rho_4 u_4 \tag{6}$$

Assuming that the flow properties in regions 3 and 4 are related through the isentropic relations, we have

$$\delta\rho/\rho = (1/\gamma)(\delta p/p) \tag{7}$$

Writing Eq. (6) in small-disturbance notation, neglecting the product of two primed quantities, and using Eq. (7) results in the following:

$$p_3'/p_1 + \gamma(u_3'/u_1) - p_4'/p_1 - \gamma(u_4'/u_1) = 0 \tag{8}$$

Writing a statement of the first law of thermodynamics for a control volume about the cascade blade passage (neglecting the volume of the blade passage), assuming the properties in regions 1–4 are related through isentropic processes, and using the small-disturbance assumption results in the following:

$$p_3'/p_1 + \gamma M_{x1}^2(u_3'/u_1) - p_4'/p_1 - \gamma\left(M_{x1}^2 \cos^2\Gamma\right)(u_4'/u_1) = 0 \tag{9}$$

Note that a $\cos^2\Gamma$ appears in the denominator of the right-hand term of Eq. (9) because of flow observation (8).

Applying Eq. (1) to the right-running transmitted disturbance and using the observation that this disturbance propagates along the blade passage (the flow before and after the transmitted disturbance is aligned with the blade passage) results in the following:

$$p_4'/p_1 - \gamma(M_{x1}/\cos\Gamma)(u_4'/u_1) = 0 \tag{10}$$

Equations (5) and (8–10) form a system of four linear equations for the unknowns:

$$p_3'/p_1, \qquad u_3'/u_1, \qquad p_4'/p_1, \qquad u_4'/u_1$$

If a response coefficient R is defined to be the ratio of the reflected disturbance pressure change to the incident disturbance pressure change,

$$R = \left(\frac{p_3'}{p_1} - \frac{p_2'}{p_1}\right) \Bigg/ \left(\frac{p_2'}{p_1}\right) = \frac{p_3 - p_2}{p_2 - p_1}$$

Solving the four linear equations for the response coefficient yields

$$R = \tan^2\left(\frac{\Gamma}{2}\right)\left(\frac{1 + M_{x1}}{1 - M_{x1}}\right) \tag{11}$$

Supersonic Mach Number

From the flow observation that if the flow is supersonic, all turning to align the flow with the blade passage occurs upstream of the blade passage, $u_3'/u_1 = 0$. From Eq. (5), if $u_3'/u_1 = 0$,

$$p_3'/p_1 = 2(p_2'/p_1) \tag{12}$$

Because, for the subsonic case, $u_3'/u_1 \geq 0$, this limits the response coefficient to $R \leq 1.0$. If $R = 1.0$, $u_3'/u_1 = 0$. This condition is a constant-velocity outflow condition at the face of the cascade. If the total Mach number in the blade passage is greater than or equal to 1 ($M_{x1}/\cos\Gamma \geq 1.0$), then

$$R = 1.0 \tag{13}$$

Discussion

The response coefficient is predicted from Eq. (11) for subsonic flow and Eq. (13) for supersonic flow. Small-disturbance model results are compared with cascade Euler results in Fig. 6. The agreement is encouraging.

Also shown are data from an experiment[8,9] whose purpose was to measure the response when an upstream acoustic disturbance was reflected from the face of a compressor. Response coefficient data from the experiment are shown in Fig. 6. for axial Mach numbers of 0.1 and 0.184. Response coefficients were computed using the peak amplitudes of the incident and reflected pressure waves. A horizontal bar and symbols spanning a range of stagger angles from 45 to 60 deg were used to represent the data in Fig. 6 because of the hub-to-tip variation in the stagger angle for the compressor used in the experiment. Agreement between the small-disturbance model and the experiment is also encouraging.

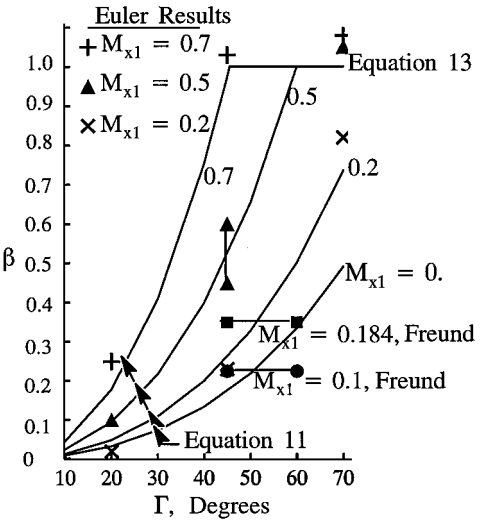

Fig. 6 Comparison of small disturbance model results and Euler results for the response coefficient.

Data from the experiment of Ref. 9 also showed reflection responses from downstream stages of the compressor. These downstream responses are expected to disappear with increasing axial Mach number. The data reported in Fig. 6 are for the reflection response from the first stage of the compressor.

New Outflow Boundary Condition from the Small-Disturbance Model

The goal is to provide the correct physical behavior with a simple numerical boundary-condition scheme that does not require a significant increase in computer resources. A characteristic approach suggested by Hankey[15] was selected for this purpose because it is relatively simple and because the level of approximation used is consistent with the analysis approximations of the preceding small-disturbance analysis. Incident, transmitted, and reflected disturbances and the respective flow regions defined in Figs. 4 and 5 are shown in an x–t diagram in Fig. 7.

Following Hankey,[15] viscous effects are neglected in the boundary-condition formulation although the boundary condition is to be used for both viscous and inviscid flows. The error introduced by neglect of viscous effects over one cell is minor. A second assumption is that the flow is locally one dimensional near the outflow boundary. This is usually approximately correct because the flow-duct area variation near the boundary is usually minor. The one-dimensional Euler equations can be stated as follows:

$$\begin{bmatrix} \rho \\ \rho u \\ \rho e \end{bmatrix}_t + \begin{bmatrix} \rho u \\ \rho u^2 + p \\ \rho u H \end{bmatrix}_x = 0 \tag{14}$$

where $H = e + p/\rho = [a^2/(\gamma - 1)] + u^2/2$.

Equation (14) can be expressed in terms of new dependent variables q, r, and s. Assuming small perturbations, linearizing, and using the subscript 1 to indicate a reference state about which a perturbation occurs yields the following:

$$\begin{bmatrix} q \\ r \\ s \end{bmatrix}_t + \begin{bmatrix} u_1 + a_1 & 0 & 0 \\ 0 & u_1 - a_1 & 0 \\ 0 & 0 & u_1 \end{bmatrix} \begin{bmatrix} q \\ r \\ s \end{bmatrix}_x = 0 \tag{15}$$

where $q = u + (a_1/\gamma)\ell n p$, $r = u - (a_1/\gamma)\ell n p$, and $s = (1/\gamma)\ell n p - \ell n \rho$.

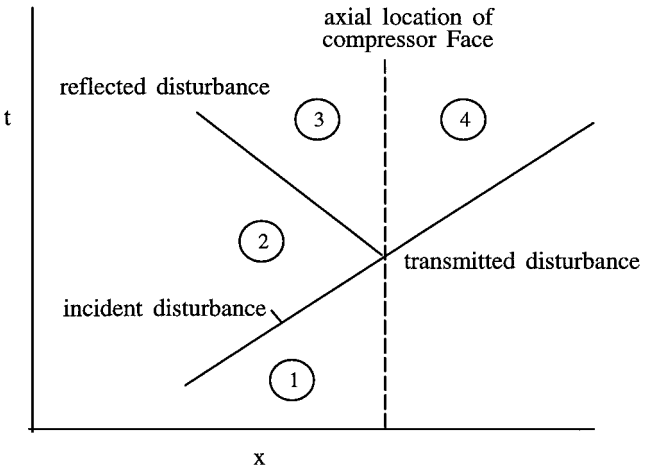

Fig. 7 Diagram (x–t) of the reflection of an acoustic disturbance from the compressor face.

Equation (15) can be expanded to yield the following:

$$q_t + [u_1 + a_1]q_x = 0 \tag{16}$$

$$r_t + [u_1 - a_1]r_x = 0 \tag{17}$$

$$s_t + [u_1]s_x = 0 \tag{18}$$

Equations (16–18) are the linearized Euler equations in characteristic form. Because Eq. (16) is a total differential along lines with slope $dx/dt = u_1 + a_1$, then q is invariant along those lines. Similarly, r and s are invariant along lines with slopes $dx/dt = u_1 - a_1$ and $dx/dt = u_1$. The coefficients, $u_1 + a_1$, $u_1 - a_1$, and u_1 are the characteristics of the Euler equations. The equations with coefficients $u_1 + a_1$ and u_1 describe propagation of information out of the inlet (the solution domain). The equation with the $u_1 - a_1$ coefficient describes propagation of information into the domain for a subsonic flow. The boundary condition should, thus, satisfy Eqs. (16) and (18). Equation (17) is replaced with the condition one wishes to satisfy on the boundary in the boundary-condition specification.

At the outflow boundary, the propagation of disturbances from the inlet results in changes in q and s with respect to time. When these disturbances interact with the compressor, changes in r with respect to time are generated. This suggests a functional relationship exists between changes in r on the boundary with respect to time and changes with respect to time in q and s. In equation form, this hypothesis can be written

$$r_t = F(q_t, s_t)$$

If the responses to convective temperature and acoustic disturbances are assumed to be additive in a simple linear way (an infinite variety of assumptions could be made about the form of this relationship),

$$r_t = -\beta q_t - \xi s_t$$

where the minus signs in the preceding relationship are arbitrary. When just a convective density disturbance was considered by Paynter,[11] the outflow boundary was found to be nonreflective, which implies $\xi = 0$. This suggests that

$$(r + \beta q)_t = 0 \tag{19}$$

The equations solved on the boundary in characteristic variable form are, thus,

$$\begin{bmatrix} q \\ (r + \beta q) \\ s \end{bmatrix}_t + \begin{bmatrix} u_1 + a_1 & 0 & 0 \\ 0 & 0 & 0 \\ 0 & 0 & u_1 \end{bmatrix} \begin{bmatrix} q \\ (r + \beta q) \\ s \end{bmatrix}_x = 0 \tag{20}$$

Because $dx/dt = 0$ on the boundary, $r + \beta q$ is a Reimann invariant on the boundary.

The cascade analysis by Paynter[11] found that the reflection response to an acoustic disturbance was a function of the local flow properties just upstream of the cascade and the blade geometry. This suggests that β is a function of these parameters. Function β will be related to the response coefficient from the small-disturbance analysis and to the change in pressure on the boundary with respect to time expressed in a finite difference form to complete the boundary-condition formulation.

Substituting the definitions of q and r into Eq. (19) and expanding yields

$$u_t - (a_1/\gamma p_1)p_t = -\beta[u_t + (a_1/\gamma p_1)p_t]$$

Rearranging, we have

$$u_t = (a_1/\gamma p_1)[(1 - \beta)/(1 + \beta)]p_t \tag{21}$$

Equation (21) is the condition that is to be satisfied on the boundary in conjunction with Eqs. (16) and (18). Rewriting Eq. (16) using the definition of q, we have

$$u_t + (a_1/\gamma p_1)p_t + [u_1 + a_1][u_x + (a_1/\gamma p_1)p_x] = 0 \tag{16a}$$

Substitution of Eq. (21) into Eq. (16a) results in the following:

$$(a_1/\gamma p_1)[(1 - \beta)/(1 + \beta)]p_t + (a_1/\gamma p_1)p_t + [u_1 + a_1][u_x + (a_1/\gamma p_1)p_x] = 0 \tag{22}$$

For a right-running acoustic disturbance propagating into a uniform flow, a change in pressure can be related to a change in velocity by using information about the Riemann invariants along the left-running characteristics. Because the Riemann invariants of the left-running characteristics are constant across the right-running characteristic because they originate in a region of uniform flow,

$$r(x, t) = u - (a_1/\gamma)\ln p = \text{const}$$

Differentiating with respect to x and rearranging, we have

$$u_x = (a_1/\gamma)\ln p_x \tag{23}$$

Substituting Eq. (23) into Eq. (22) and rearranging, we have

$$p_t = -(u_1 + a_1)(1 + \beta)p_x \tag{24}$$

Equation (24) has the form of a one-dimensional wave equation. A stable explicit numerical scheme with truncation error $\mathcal{O}(\Delta t, \Delta x)$ for the static pressure on the boundary at time step $n + 1$, in terms of known conditions at time step n, can be obtained if backward difference expressions are used in both space and time. Other difference expressions could have been chosen. The intent was to show that a reasonable boundary condition could be formulated:

$$p_i^{n+1} = p_i^n + (1 + \beta)\left(p_{i-1}^n - p_i^n\right)\left[u_i^n + a_i^n\right](\Delta t/\Delta x) \tag{25}$$

If the Courant number is defined as

$$\sigma = \left[u_i^n + a_i^n\right](\Delta t/\Delta x)$$

the final difference expression for pressure is

$$p_i^{n+1} = p_i^n + (1 + \beta)\sigma\left(p_{i-1}^n - p_i^n\right) \tag{26}$$

The β parameter must be related to the response coefficient R to use the small-disturbance analysis for R in an outflow boundary condition. Suppose an acoustic disturbance is propagating toward the outflow boundary. If at time step n, the disturbance is at the $i - 1$ axial grid point, the disturbance will propagate from cell $i - 1$ to cell i (the outflow boundary) if $\sigma = 1.0$. Rewriting Eq. (26) in small-disturbance notation yields

$$p_3 = p_1 + (1 + \beta)(p_2 - p_1)$$

or, from a comparison of the preceding expression with that for the response coefficient R it is clear that $\beta = R$:

$$\beta = (p_3 - p_2)/(p_2 - p_1)$$

The actual boundary condition is specification of the solution vector variables at time step $n+1$ at the boundary, axial station i. These vector variables are as follows:

$$\rho_i^{n+1}, \qquad (\rho u)_i^{n+1}, \qquad (\rho e)_i^{n+1}$$

The velocity on the boundary at time step $n+1$ is found from Eqs. (21) and (26):

$$u_i^{n+1} = u_i^n + \left(a_i^n \middle| \gamma p_i^n\right)(1-\beta)\sigma\left(p_{i-1}^n - p_i^n\right) \tag{27}$$

Equation (18) can be expanded in finite difference formulation to achieve the desired expression for density:

$$\rho_i^{n+1} = \rho_i^n + \sigma\left[\frac{M_i^n}{M_i^n+1}\left(\rho_{i-1}^n - \rho_i^n\right) + \rho_i^n \frac{\left(\beta M_i^n + \beta + 1\right)}{\gamma\left(M_i^n+1\right)p_i^n}\left(p_{i-1}^n - p_i^n\right)\right] \tag{28}$$

Combining Eqs. (27) and (28) yields

$$(\rho u)_i^{n+1} = \left[(\rho a)_i^n (1-\beta)\sigma \middle| \gamma\right]\left[\left(p_{i-1}^n - p_i^n\right) \middle| p_i^n\right] + \rho_i^{n+1} u_i^n \tag{29}$$

From the definition of internal energy,

$$(\rho e)_i^{n+1} = (\rho e)_i^n + \left[\left(u_i^n\right)^2 \middle| 2\right]\left(\rho_i^{n+1} - \rho_i^n\right) + \sigma\left[(1+\beta)/(\gamma-1) + M_i^n(1-\beta)\right]\left(p_{i-1}^n - p_i^n\right) \tag{30}$$

Equations (28–30) define the solution vector variables on the boundary at time step $n+1$.

Note that, if $\beta = 1.0$, Eq. (26) gives a pressure change consistent with a constant velocity outflow boundary condition. If $\beta = 0$, the boundary condition is nonreflective. If $\beta = -1.0$, a constant-pressure boundary condition is obtained.

Results

The accuracy of the new outflow boundary condition can be evaluated for both acoustic and convective disturbances by comparing the values of pressure and density from Eqs. (26) and (28) after the reflection of a disturbance from the boundary with analytic results, the Euler results of Paynter,[11] and results from the Freund and Sajben[8,9] compressor experiment.

Analytic Checks

Consider first an acoustic disturbance that is a step 1% increase in pressure propagating downstream in a constant-area duct at an initial Mach number of 0.4. Assume that the disturbance interacts with an unloaded cascade with a blade stagger angle of 70 deg. From Fig. 6, using the Euler cascade analysis results,[11] $p_3/p_1 = 1.02$. Because the reflection of the disturbance is isentropic, $\rho_3/\rho_1 = 1.01425$. From Eq. (26), $p_i^{n+1}/P_I^n = 1.02$ assuming a time step such that the disturbance propagates from one cell off the boundary to the boundary, $i-1$ to i ($\sigma = 1.0$). From Eq. (28), $\rho_i^{n+1}/\rho_i^n = 1.014283$. The error in pressure is, thus, 0% and the error in density is 0.004%.

For a convective temperature disturbance, from Ref. 11, $p_3/p_1 = p_2/p_1 = 1.0$ and $\rho_3/\rho_1 = \rho_2/\rho_1$. From Eqs. (26) and (28), it is clear that pressure and density on the boundary would be computed without error provided $\sigma M_{x1}/(M_{x1}+1) = 1.0$. If $\sigma = 1.0$, which would be the normal upper limit on the time step, the convective disturbance has not propagated from $i-1$ to i, but has only covered a fraction of the distance. Thus, for a step change disturbance, two (or more) time steps would be required to compute the change in density.

One-Dimensional Euler Results

The new boundary condition was implemented in two one-dimensional Euler codes.[12,13] Simulation results[12] are shown in Fig. 8 for a step change acoustic disturbance ($\delta p/p = 0.046$) in a constant-area channel with an axial Mach number of 0.3, interacting with the outflow boundary. Pressure distributions in the duct are plotted in Fig. 8 at uniform time increments to show the effect of the response coefficient on the strength of the reflected pressure disturbance. Pressure–time data are plotted for response coefficient β values of 0., 0.5, and 1.0 in the plot. The new boundary condition performs as expected.

Comparison of One-Dimensional Euler Results and Experimental Results

The Ref. 9 compressor experiment was conducted in a facility that combined a constant-area annular inlet with the compressor from a multistage General Electric T58-3 helicopter engine with the power turbine removed. The turbine was driven using high-pressure air from an external source that limited the Mach number that could be obtained in the inlet to about 0.2.

Acoustic expansion pulses were generated from the sudden collapse of a flexible boot positioned approximately midway along the annulus. A sudden collapse of the boot created two expansion wave pulses, one traveling upstream and one traveling downstream. The test facility and the locations of the four pressure transducers used to record the passage of acoustic waves are shown schematically in Fig. 9 (from Fig. 6 of Ref. 9).

The LAPIN code[13] was used to simulate the compressor experiment for an inlet condition of Mach 0.17 (Fig. 6 of Ref. 9). Typically used boundary conditions of constant pressure, constant Mach number, and constant velocity were investigated, as well as the new small-disturbance outflow boundary condition, to see how well they represent the response of the T58 compressor. The figure of merit for the comparison is the pulse that is reflected back upstream from the compressor face. The reflected pulse was determined for all cases by using the procedure explained in Ref. 9. The procedure involves a time shift of the incident pulse time history from station 1 to station 4 (Fig. 9). (Although not shown, LAPIN accurately simulated the incident pulses as stations 1, 2, and 3.) At station 4 the incident and reflected pulses overlap. The reflected pulse is obtained by subtracting the station 1 time-shifted history from the time history at station 4. The simulation results for the various boundary conditions are compared with the experimental data in Fig. 10. Note again that the incident pulse is an expansion wave. The minimum peak for the incident disturbance was about −3.8% of the initial steady-state pressure (Fig. 6 of Ref. 9). The pulse reflected from the T58 is also an expansion wave but with a much smaller amplitude of about −1.3%. As expected, the constant-pressure outflow boundary condition results in a reflected wave of opposite sign to the incident wave. If the duct area were constant all of the way to the compressor face, the reflected pulse amplitude should equal the incident pulse amplitude. However, the duct converges near the compressor face so that the reflected pulse amplitude is less than that of the incident pulse. The constant-pressure boundary condition would obviously be a poor choice to represent the reflection of an acoustic disturbance from a compressor. The constant-Mach-number and constant-velocity outflow boundary conditions result in responses of the correct sign, but overpredict the amplitude by a factor of two or more. The new small-disturbance boundary condition results in a reflected pulse that has the correct sign and approximately the correct amplitude. The response coefficient β used with the boundary condition was 0.362 based on the T58 first-stage-rotor midspan stagger angle of 52 deg and an undisturbed Mach number at the compressor face of 0.2067. This boundary condition simply simulates a single blade row. That is, for the T58 case it ignores the variable inlet guide vanes and the multiple blade rows downstream of the first-stage rotor, thought to be responsible for subsequent peaks observed in the experimental reflected pulse.[9] Still, the new boundary condition offers a significant improvement in accuracy for the amplitude of the reflected pulse relative to the other typically used boundary conditions.

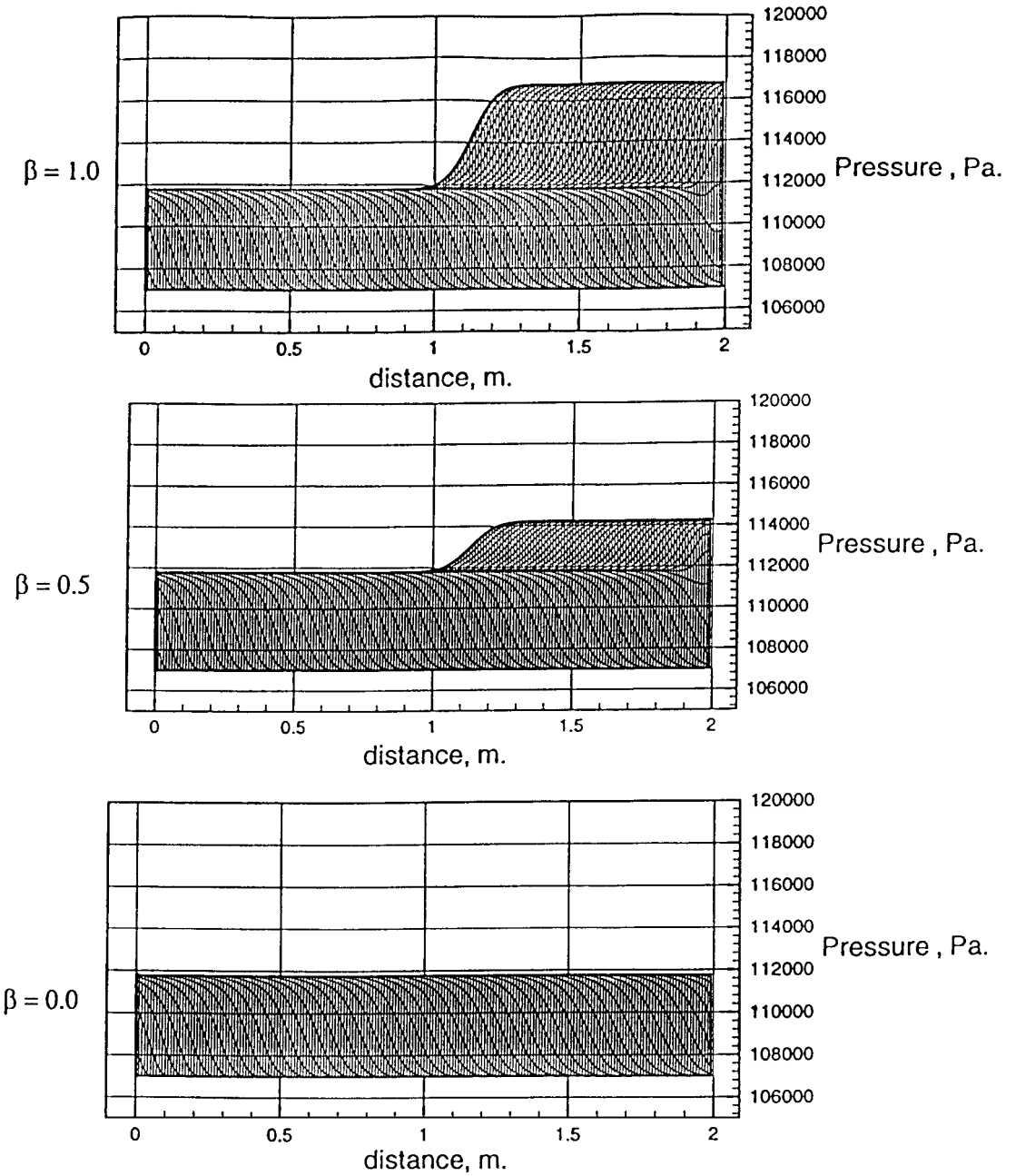

Fig. 8 Reflection of a step in pressure acoustic disturbance for different values of β.

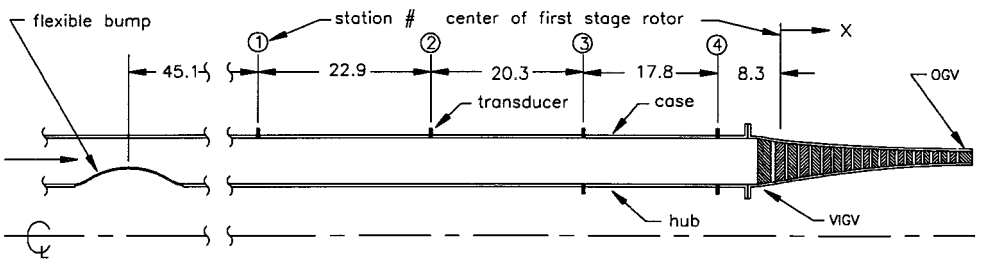

Fig. 9 Apparatus for the compressor experiment of Freund and Sajben.[8,9]

Example Application

Simulation of a supersonic mixed-compression inlet flow was used to demonstrate how the predicted tolerance to unstart depends on the outflow boundary condition. LAPIN was used for the inlet simulations. Results are compared for the new small-disturbance boundary condition and the typically used constant-velocity, constant-Mach-number, and constant-pressure boundary conditions. The inlet studied was designed for Mach 2.5 operation, optimized experimentally, and tested both steady state and dynamically.[16] The inlet was sized for operation with and tested with a GE J85-13 turbojet engine.

The simulated inlet was scaled by a factor of three to give results representative of a full-scale system. The operating point conditions were $M = 2.5$, altitude $= 65{,}000$ ft, and a compressor-face Mach number of 0.3143. The corresponding compressor-face corrected airflow and total pressure recovery were 300 lbm/s and 93%

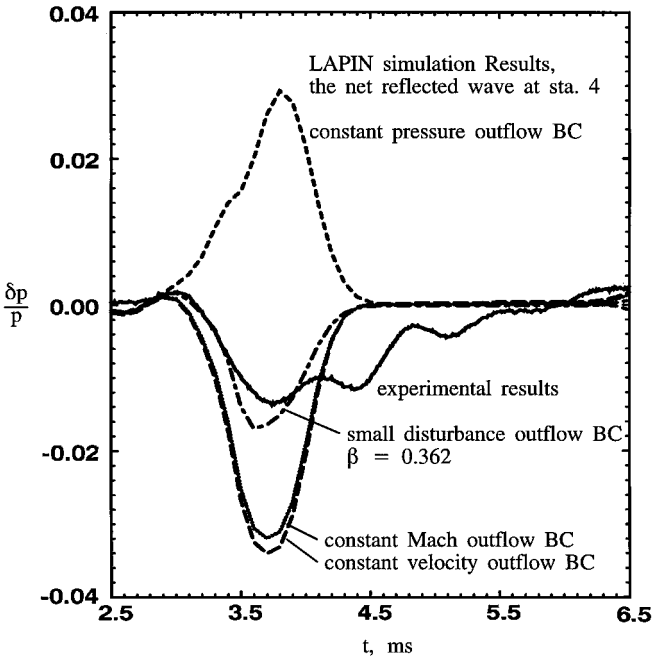

Fig. 10 Comparison of LAPIN results and experimental results.

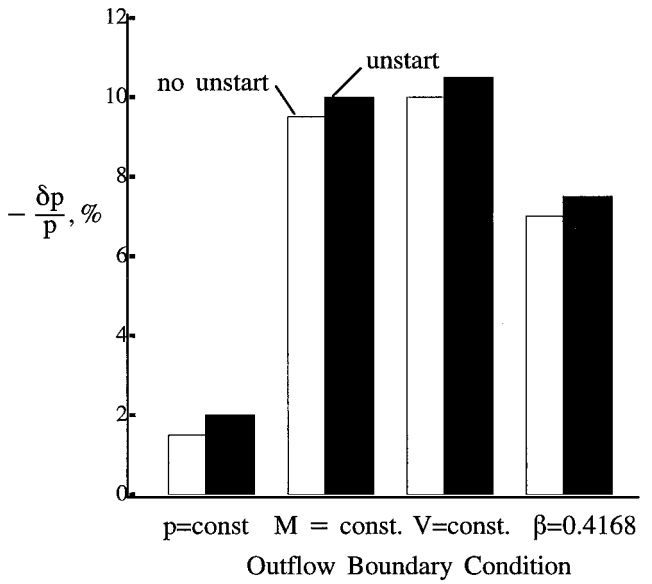

Fig. 11 Effect of the outflow boundary condition on the predicted inlet unstart tolerance: results for the NASA LERC 40–60 mixed compression inlet at $M = 2.5$.

freestream total pressure, respectively, corresponding to a stability margin of several percent. That is, the inlet could tolerate about a 9% reduction in corrected airflow without the terminal (normal) shock moving upstream of the throat and unstarting. The simulation included inlet bleeds and bypasses but no active controls.

The inlet was subjected to step decreases in freestream static pressure that occurred over one simulation time step of 0.00001 s. The result is an expansion wave that travels downstream. When it reaches the normal shock, the shock responds by moving upstream an identical distance regardless of the outflow boundary. The perturbation continues downstream and is reflected back upstream from the outflow boundary. When it reaches the normal shock, the reflected wave will increase or decrease the upstream shock displacement depending on whether the reflection is a compression wave or an expansion wave, respectively. To determine the unstart tolerance, the perturbation amplitude was changed in increments of 0.5%. This allowed the onset of unstart to be bracketed to within 0.5%. Results from these simulations are shown in Fig. 11 and indicate that the outflow boundary condition has a strong effect on the strength of the disturbance needed to induce an unstart. As expected, use of the constant-pressure boundary condition results in the lowest predicted unstart tolerance, between −1.5 and −2%, because the expansion wave is reflected as a compression wave. The tolerance is substantially lower than that predicted with the proposed new small-disturbance model. In these simulations the small-disturbance boundary condition used a response coefficient of 0.4168 based on the J85 first-stage-rotor midspan stagger angle of 50 deg and the undisturbed compressor-face Mach number of 0.3143. The constant-Mach-number and constant-velocity boundary conditions overpredict the unstart tolerance by about 40% relative to the small-disturbance boundary condition.

The results of Figs. 10 and 11 illustrate the importance of selecting a correct outflow boundary condition, particularly from an inlet controls perspective. Using a boundary condition that predicts a tolerance to unstart that is too low may result in the inlet being controlled at an inefficient operating condition to assure operability. If the predicted inlet tolerance is too high, the inlet control might be designed such that excessive unstarts would occur. The new small-disturbance boundary condition is thought to provide the most accurate short-term compressor response and, therefore, the best prediction of inlet unstart tolerance.

Conclusions

The process for alignment of the flow with the blade passage (after an acoustic disturbance has caused a misalignment) depends on whether the flow in the blade passage prior to the disturbance is subsonic or supersonic. If the flow is subsonic, realignment starts with the passage of the flow through the reflected disturbance but is completed within the blade passage. If the flow is supersonic, all realignment occurs through the disturbance reflected from the cascade ahead of the blade passage.

A small-disturbance model was formulated for the response from a cascade of a downstream propagating acoustic disturbance. Model results agree well with Euler analysis results from Ref. 11 and with the available experimental data.

The small-disturbance response model was then used to formulate a new one-dimensional outflow characteristic boundary condition for acoustic disturbances that satisfies at least simple checks on the accuracy of the boundary condition for acoustic and convective density disturbances.

The new outflow boundary condition was implemented in two one-dimensional Euler codes. Simulation results indicate that the boundary condition performed as expected for the compressor experiment of Freund and Sajben.[8,9] Simulation results also demonstrated the importance of the outflow boundary condition to the prediction of inlet normal-shock response and unstart tolerance for a supersonic mixed compression inlet.

Acknowledgments

The authors would like to thank S. F. Birch, R. Decher, D. D. Knight, D. W. Mayer, and M. Sajben for their comments on the work and for reviewing the manuscript, as well as D. Freund for providing preliminary data from his thesis project.

References

[1]Hedges, L., Lewis, J., Carlin, C., and Beck, C., "Supersonic Inlet Simulations with Closed Loop Control and Moving Control Surfaces," AIAA Paper 96-0493, Jan. 1996.

[2]Cole, G. L., Melcher, K. J., Chicatelli, A. A., Hartley, T. T., and Chung, J. K., "Computational Methods for HSCT-Inlet Controls/CFD Interdisciplinary Research," AIAA Paper 94-3209, June 1994.

[3]Mayer, D. W., and Paynter, G. C., "Prediction of Supersonic Inlet Unstart Caused by Freestream Disturbances," *AIAA Journal*, Vol. 33, No. 2, 1995, pp. 256–275.

[4]Chung, J., and Cole, G. L., "Comparison of Compressor Face Boundary Conditions for Unsteady CFD Simulations of Supersonic Inlets," AIAA Paper 95-2627, July 1995.

[5]Clark, L. T., "Dynamic Response Characteristics of a Mixed Compression Supersonic Inlet as Part of a Larger System," AIAA Paper 95-0036, Jan. 1995.

[6]Chung, J. K., "Numerical Simulation of a Mixed Compression Supersonic Inlet Flow," AIAA Paper 94-0583, Jan. 1994.

[7]Decher, R., Mayer, D. W., and Paynter, G. C., "On Supersonic Inlet-Engine Stability," AIAA Paper 94-3371, June 1994.

[8]Freund, D. D., and Sajben, M., "Experimental Investigation of Outflow Boundary Conditions Used in Unsteady Inlet Flow Computations," AIAA Paper 97-0610, Jan. 1997.

[9]Freund, D., and Sajben, M., "Reflection of Large Amplitude Acoustic Disturbances from an Axial Compressor," AIAA Paper 97-2879, July 1997.

[10]Cooper, G. K., and Sirbaugh, J. R., "The PARC Code: Theory and Usage," Arnold Engineering Development Center, AEDC-TR-89-15, Arnold AFB, TN, Dec. 1989.

[11]Paynter, G. C., "Response of a Two-Dimensional Cascade to an Upstream Disturbance," *AIAA Journal*, Vol. 35, No. 3, 1997, pp. 434–440.

[12]Boris, J. P., Landsberg, A. M., Oran, E. S., and Gardner, J. H., "LCPFCT—A Flux Corrected Transport Algorithm for Solving Generalized Continuity Equations," Naval Research Lab., NRL/MR/6410-93-7192, Washington, DC, April 1993.

[13]Varner, M. O., Martindale, W. R., Phares, W. J., Kneile, K. R., and Adams, J. C., Jr., "Large Perturbation Flow Field Analysis and Simulation for Supersonic Inlets," NASA CR-174676, Sept. 1984.

[14]Shapiro, A. H., *The Dynamics and Thermodynamics of Compressible Fluid Flow*, Vol. 2, Ronald, New York, 1954, p. 918.

[15]Hankey, W. L., "Introduction to Computational Aerodynamics," U.S. Air Force Wright Aeronautical Labs., AFWAL-TR-3031, Wright Field, OH, April 1983.

[16]Wasserbauer, J. F., "Dynamic Response of a Mach 2.5 Axisymmetric Inlet with Engine or Cold Pipe and Utilizing 60 Percent Internal Area Contraction," NASA TN D-5338, July 1969.

D. S. McRae
Associate Editor